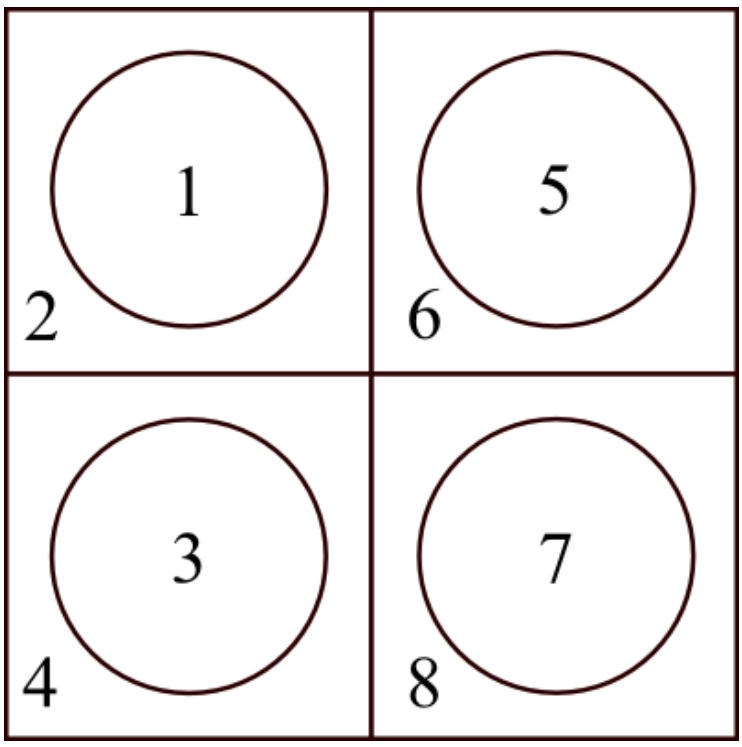
CHALMERS



Development of a hybrid neutron transport method in 2 energy groups

SEBASTIAN CARBOL
Department of Physics
Chalmers University of Technology
Gothenburg, Sweden 2017
CTH-NT-326

Acknowledgements

I would like to thank my supervisor Christophe Demazière for his help and understanding throughout the work. I would also like to thank Mikael Andersson for his contributions that were supported by the NKS and also Klas Jareteg for his good advice and help.

Abstract

A new hybrid neutron transport method was developed and implemented using the response matrix formulation. The method combines the advantages of deterministic and probabilistic modelling, namely the flexibility in modelling any geometry with high accuracy and the low computing cost of the hybrid scheme. The probabilities associated with the response matrix formulation were determined using the Monte-Carlo based code Serpent2. Further a deterministic code was written to solve for the neutron flux using the response matrix method.

With some modifications to Serpent2 the needed probabilities could be determined and a converged neutron flux solution was achieved, for a simplified BWR fuel assembly, using the written deterministic code.

Contents

1 Introduction **1**
1.1 Purpose . . . 2
1.2 Aim . . . 2
1.3 Literature study . . . 2

2 Theory **4**
2.1 Derivation for the response matrix formulation . . . 4
2.1.1 Local problem . . . 6
2.1.2 Global problem . . . 8
2.2 Response matrix formulation . . . 11
2.3 Power iteration method . . . 12

3 System **15**
3.1 Assembly system . . . 15
3.2 Fuel pin system . . . 16

4 Implementation **19**
4.1 Calculating probabilities in Serpent2 . . . 19
4.1.1 Neutrons entering through a surface . . . 20
4.1.2 Neutrons emitted from a region . . . 22
4.2 Labelling the system . . . 24
4.3 Structure of deterministic MatLab code . . . 26
4.4 Building response matrix R . . . 27
4.5 Building P matrix . . . 28
4.6 Building the S matrix . . . 29
4.7 Calculating the F matrix . . . 31
4.8 Calculating emission density . . . 32
4.9 Calculating source currents . . . 32
4.10 Calculating source flux . . . 33
4.11 Cross-section data . . . 33

5 Results and discussion **34**
5.1 Probabilities . . . 34
5.2 Neutron flux . . . 37
5.3 Conclusion and outlook . . . 40

6 Bibliography **41**

1 Introduction

With the threat of global warming increasing the need for electricity production without emission of greenhouse gases is becoming more needed. In countries such as Sweden and France, nuclear power contributes up to 45 % and 75 % of the total electricity production respectively [1][2]. However, for the further use and expansion of nuclear power to become encouraged the safety of operations must be proven and this may be done using advanced modelling techniques. These modelling techniques are used to predict and model important parameters and the behaviour of the nuclear reactor core. At the moment two major methods prevail: deterministic and probabilistic (Monte Carlo) [3].

A nuclear reactor is a unique system and modelling its behaviour is difficult due to the multi-physics and multi-scale properties. In order to completely determine the physical behaviour of the reactor the neutron density field, the fuel temperature and the coolant field need to be modelled and coupled to each other. Often modelling these different fields is not sufficient and the different scales of the system need to be modelled as well, going from pin cell level to fuel assembly level.

Deterministic modelling techniques are based on solving the neutron transport equation (the Boltzmann equation) explicitly. The neutron transport equation is very complicated and may only be solved using approximations in order to reduce the complexity of the problem. The difficulties in solving the neutron transport equation lies in the multi-physics and multi-scale nature of a nuclear reactor as well as the large number of unknowns. Hence it is solved using space-homogenisation, energy-discretisation and angular discretisation techniques. Deterministic modelling methods are generally fast and require reasonable computer resources, but the disadvantage is that the codes are constructed for a fixed geometry or reactor type.

The probabilistic methods solve the neutron transport by modelling a single neutron at a time, tracking its path as it interacts in the geometry of the problem. The neutrons are tracked and each happening is predicted by probabilities determined from the energy-dependent microscopic cross-sections of the materials present. Following a large number of neutron histories and using statistical averages the general behaviour of the core may be determined. These types of calculations are computer intensive and are used to set benchmark solutions to specific problems [4].

There are possibilities to combine probabilistic Monte Carlo methods with deterministic methods to have a ”hybrid” method. This type of approach would combine the benefits of each method, fast computational time from the deterministic approach and higher accuracy thanks to the probabilistic approach. Work has previously been done with using hybrid approaches such as using it to speed up the k eigenvalue convergence using Monte Carlo Coarse Mesh Finite-Differences (MC-CMFD) [5]. This type of projects have had success and hence it is interesting to look at further hybrid approaches.

1.1 Purpose

1.2 Aim

The aim of the master thesis is to combine deterministic and probabilistic modelling and produce a code that can model the neutron behaviour in a 2D nuclear reactor core using the response matrix method. This will be done by first determining the required probabilities needed using a Monte Carlo code. Secondly by producing a code to implement the response matrix method using the produced collision probabilities and lastly to investigate the accuracy and reliability of the computer code.

1.3 Literature study

There has been previous work done on hybrid neutron transport methods and one of the more extensive works is the Coarse Mesh Radiation Transport method (COMET) by Dingkang Zhang and Farzad Rahnema [6] based on the previous work done by Scott Mosher and Farzad Rahnema [7]. In the COMET method the spatial domain is divided up into a number of coarse meshes. Instead of solving the whole-core transport equation a set of local fixed source problems are solved instead. These local problems can be determined using response functions. These response functions are determined using Monte-Carlo simulations since they are only dependent on the coarse mesh and the material compositions. Libraries of response functions are created for each mesh and also for some defined effective multiplication factors. Using interpolation these libraries can be used for any effective multiplication factor. Once these libraries are determined a deterministic solver is used to get the whole-core solution to the problem which has the following algorithm:

1. Initial guess of the $k_{effective}$ and the incoming neutron currents.
2. Update the response functions for the updated eigenvalue.
3. Perform inner iterations to get the new incoming neutron currents.
4. Use a neutron balance equation to update the eigenvalue.
5. Repeat steps 2-4 until convergence.

This method is similar to pre-existing deterministic methods in the sense that it uses a pre-computed library, similar to precomputed homogenised cross-sections, however, this method still uses the heterogeneity of the reactor core. In this way the method is able to have an accuracy close to Monte-Carlo but with three orders of magnitude faster computational speed.

Further hybrid methods have been used by M. J. Lee et al. in their work on "Coarse mesh finite difference formulation for accelerated Monte Carlo (MC) eigenvalue calculation" where they use a deterministic scheme to faster update the fission source distribution (FSD) [5]. Firstly the coarse mesh finite difference (CMFD) system is built up by the use of MC tallies to create coarse mesh homogenisation parameters. Next the CMFD eigenvalue problem is solved through a deterministic method and the feedback to the MC method is given by a weight adjustment scheme to the MC FSD. The complete scheme may be seen in figure 1 below:

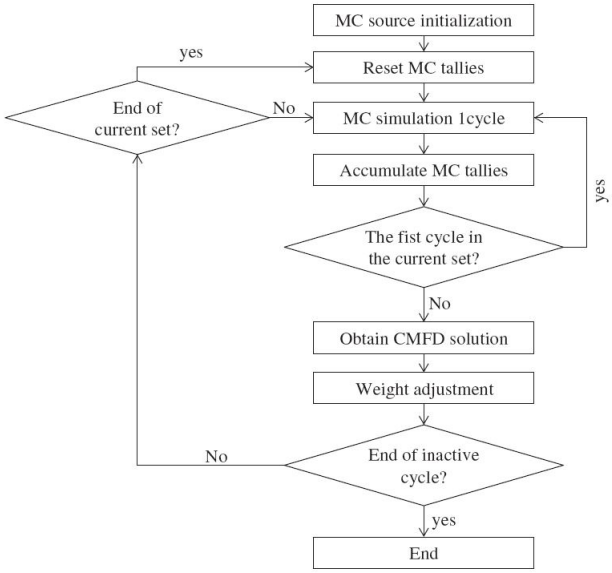


Figure 1: The MC-CMFD iteration scheme [5].

This method had success and was able to reduce the number of inactive cycles in the MC to 20 from 600 with the same accuracy, for a simple test problem. Further the results could be made more accurate and reliable if the MC-CMFD feedback was given to the active cycles as well.

2 Theory

In this work, a different approach is used as a hybrid solution, making use of the so-called response matrix formulation.

2.1 Derivation for the response matrix formulation

The derivation of the equations used in the response matrix formulation are based on the integro-differential steady state (S.S) Boltzman transport equation given below:

$$\bar{\Omega} \cdot \bar{\nabla}\Psi(\bar{r},\bar{\Omega},E) + \Sigma_T(\bar{r},E)\Psi(\bar{r},\bar{\Omega},E) = q(\bar{r},\bar{\Omega},E) \tag{1}$$

The emission density q is given by:

$$q(\bar{r},\bar{\Omega},E) = \int_{4\pi}\int_0^\infty \Sigma_s(\bar{r},\bar{\Omega}' \to \bar{\Omega},E' \to E)\Psi(\bar{r},\bar{\Omega}',E')d\omega' dE' + \frac{\chi(E)}{4\pi k}\int_0^\infty \nu(E')\Sigma_f(\bar{r},E')\phi(\bar{r},E')dE' \tag{2}$$

where:

$$\chi(E) = \chi^p(E)(1-\beta) + \sum_{i=1}^{6}\chi_i^d(E)\beta_i$$

Equation 1 may be rewritten for a given direction $\bar{\Omega}_m$:

$$\bar{\Omega}_m \cdot \bar{\nabla}\Psi(\bar{r},\bar{\Omega}_m,E) + \Sigma_T(\bar{r},E)\Psi(\bar{r},\bar{\Omega}_m,E) = q(\bar{r},\bar{\Omega}_m,E) \tag{3}$$

A characteristic may be defined with a point N, $[N,\bar{\Omega}_m)$, along where a point M may be defined by:

$$\bar{r} = \bar{r}_0 + s\bar{\Omega}_m \tag{4}$$

where s is the abscissa describing the point M on the characteristic $[N,\bar{\Omega}_m)$. An infinitesimal displacement $\delta\bar{r}$ along the characteristic is given by:

$$\delta\bar{r} = \delta s\bar{\Omega}_m \tag{5}$$

and since $\delta\bar{r} \cdot \bar{\nabla}\Psi(\bar{r},\bar{\Omega}_m,E) = \delta\Psi(\bar{r},\bar{\Omega}_m,E)$ the first term of equation 3 may be rewritten as:

$$\bar{\Omega}_m \cdot \bar{\nabla}\Psi(\bar{r},\bar{\Omega}_m,E) = \frac{\delta\bar{r}}{\delta s} \cdot \bar{\nabla}\Psi(\bar{r},\bar{\Omega}_m,E) = \frac{\delta\Psi(\bar{r},\bar{\Omega},E)}{\delta s} \tag{6}$$

The dependence on $\bar{r}$ in equation 3 along the characteristic may be replaced by dependence on the abscissa s:

$$\frac{\delta\Psi(s,\bar{\Omega}_m,E)}{\delta s} + \Sigma_T(s,E)\Psi(s,\bar{\Omega}_m,E) = q(s,\bar{\Omega}_m,E) \tag{7}$$

Equation 7 is an inhomogeneous equation that may be solved using the method of variation of the constant. The homogeneous equation may be written as:

$$\frac{\delta\Psi(s,\bar{\Omega}_m,E)}{\delta s} + \Sigma_T(s,E)\Psi(s,\bar{\Omega}_m,E) = 0 \tag{8}$$

and hence:

$$\frac{\delta\Psi(s,\bar{\Omega}_m,E)}{\Psi(s,\bar{\Omega}_m,E)} = -\Sigma_T(s,E)\delta s \tag{9}$$

This may be integrated along the characteristic between the abscissa s_{in} (where the outer boundary intersects with the characteristic):

$$\ln\Psi(s,\bar{\Omega}_m,E) = -\int_{s_{in}}^{s}\Sigma_T(s',E)\delta s' + C \tag{10}$$

and hence:

$$\Psi(s,\bar{\Omega}_m,E) = C\cdot\exp\Big[-\int_{s_{in}}^{s}\Sigma_T(s',E)\delta s'\Big] \tag{11}$$

The general solution to the inhomogeneous equation may be written as:

$$\Psi(s,\bar{\Omega}_m,E) = C(s)\cdot\exp\Big[-\int_{s_{in}}^{s}\Sigma_T(s',E)\delta s'\Big] \tag{12}$$

To determine C(s) equation 12 may be used in equation 7 and hence C(s) fulfils the following equation:

$$\frac{\delta C(s)}{\delta s} = q(s,\bar{\Omega}_m,E)\cdot\exp\Big[-\int_{s_{in}}^{s}\Sigma_T(s',E)\delta s'\Big] \tag{13}$$

Equation 13 may be integrated between s_{in} and s:

$$C(s) = \int_{s_{in}}^{s} q(s',\bar{\Omega}_m,E)\cdot\exp\Big[\int_{s_{in}}^{s'}\Sigma_T(s'',E)\delta s''\Big]ds' + C(s_{in}) \tag{14}$$

Equation 14 and 12 may be combined to give:

$$\begin{aligned}\Psi(s,\bar{\Omega}_m,E) &= C(s_{in})\cdot\exp\Big[-\int_{s_{in}}^{s}\Sigma_T(s',E)ds'\Big]+\\ &\int_{s_{in}}^{s} q(s',\bar{\Omega}_m,E)\cdot\exp\Big[\int_{s_{in}}^{s'}\Sigma_T(s'',E)\delta s''\Big]ds'\cdot\exp\Big[-\int_{s_{in}}^{s}\Sigma_T(s',E)ds'\Big] \qquad (15)\\ = C(s_{in})\cdot\exp\Big[-\int_{s_{in}}^{s}&\Sigma_T(s',E)ds'\Big]+\int_{s_{in}}^{s} q(s',\bar{\Omega}_m,E)\cdot\exp\Big[-\int_{s'}^{s}\Sigma_T(s'',E)\delta s''\Big]ds'\end{aligned}$$

Noticing that $\Psi(s_{in},\bar{\Omega}_m,E) = C(s_{in})$, the following equation is finally obtained:

$$\begin{aligned}\Psi(s,\bar{\Omega}_m,E) &= \\ \Psi(s_{in},\bar{\Omega}_m,E)\cdot\exp\Big[-\int_{s_{in}}^{s}&\Sigma_T(s',E)ds'\Big]+\\ +\int_{s_{in}}^{s} q(s',\bar{\Omega}_m,E)\cdot\exp\Big[-\int_{s'}^{s}&\Sigma_T(s'',E)\delta s''\Big]ds'\end{aligned} \qquad (16)$$

The interface current method builds on from equation 16. In the interface current method the system is modelled on a global and a local scale.

2.1.1 Local problem

If the origin is chosen at the point of the observer, equation 16 may be rewritten:

$$\Psi(\bar{r},\bar{\Omega},E) = \Psi(\bar{r}_{in},\bar{\Omega},E)\cdot\exp\Big[-\tau(\bar{r}_{in},\bar{r},E)\Big]+\int_{s_{in}}^{0} q(\bar{r}-s'\bar{\Omega},\bar{\Omega},E)\cdot\exp\Big[-\tau(\bar{r}',\bar{r},E)\Big]ds' \qquad (17)$$

where the emission density is given by:

$$q(\bar{r},\bar{\Omega},E) = \frac{1}{4\pi}\int_0^{\infty}\Big[\Sigma_{s0}^0(\bar{r},E'\to E)+\frac{\chi(E)}{k}\nu(E')\Sigma_f(E',\bar{r})\Big]\phi(\bar{r},E')dE' \qquad (18)$$

In equation 17 the integrals of the exponentials have been replaced with the optical path length that is defined by:

$$\tau(\bar{r},\bar{r}',E) = \int_0^{s}\Sigma_T^0(\bar{r}-s'\bar{\Omega},E)ds' \qquad (19)$$

The optical path length is given by the distance travelled by a neutron times the transport corrected total cross-section.

Equation 18 may be integrated on all solid angles:

$$\int_{4\pi} \Psi(\bar{r},\bar{\Omega},E)d\omega = \int_{4\pi} \Psi(\bar{r}_{in},\bar{\Omega},E)\cdot \exp\Big[-\tau(\bar{r}_{in},\bar{r},E)\Big]d\omega + \\ + \int_{4\pi}\int_{s_{in}}^{0} q(\bar{r}-s'\bar{\Omega},\bar{\Omega},E)\cdot \exp\Big[-\tau(\bar{r}',\bar{r},E)\Big]ds'd\omega \tag{20}$$

An interface may be defined as: $\bar{r}_{in} = \bar{r} - s_{in}\bar{\Omega}$ and the infinitesimal surface element spanned by a change of the angle $\bar{\Omega}$ may be given by:

$$dS'\big|\bar{\Omega}\cdot\bar{n}\big| = s_{in}^2 d\omega = \|\bar{r}-\bar{r}_{in}\|^2 d\omega \tag{21}$$

At the point defined by $\bar{r}' = \bar{r} - s'\bar{\Omega}$ the infinitesimal volume element spanned by a change of the direction $\bar{\Omega}$ and of abscissa s' is:

$$dV' = s'^2 ds'd\omega = \big\|\bar{r}-\bar{r}'\big\|^2 ds'd\omega \tag{22}$$

Equation 21 and 22 may be used together with equation 20. Equation 21 is used to rewrite the integral over all solid angles as a surface integral whereas equation 22 is used to rewrite the double integral on all solid angles and the abscissa s length integral as a volume integral. It can also be seen that the left hand side of equation 20 is the scalar neutron flux and hence the following equation is obtained:

$$\phi(\bar{r},E) = \int_S \Psi_{in}(\bar{r}',\bar{\Omega},E)\frac{\exp\Big[-\tau(\bar{r}',\bar{r},E)\Big]}{\|\bar{r}-\bar{r}'\|^2}\cdot\big|\bar{\Omega}\cdot\bar{n}\big|dS' + \\ + \int_V q(\bar{r}',\bar{\Omega},E)\frac{\exp\Big[-\tau(\bar{r}',\bar{r},E)\Big]}{\|\bar{r}-\bar{r}'\|^2}dV' \tag{23}$$

The volume V of the system may be partitioned into sub-volumes V_i, such that $V = \bigcup_i V_i$, and the outer surface S may be partitioned into sub-surfaces S_a, such that $S = \bigcup_a S_a$:

$$\phi(\bar{r},E) = \sum_a \int_{S_a} \Psi_{in}(\bar{r}',\bar{\Omega},E)\frac{\exp\Big[-\tau(\bar{r}',\bar{r},E)\Big]}{\|\bar{r}-\bar{r}'\|^2}\cdot\big|\bar{\Omega}\cdot\bar{n}\big|dS' + \\ + \sum_i \int_{V_i} q(\bar{r}',\bar{\Omega},E)\frac{\exp\Big[-\tau(\bar{r}',\bar{r},E)\Big]}{\|\bar{r}-\bar{r}'\|^2}dV' \tag{24}$$

Equation 24 may be multiplied by the transport-corrected total macroscopic cross-section and integrated on a volume V_j:

$$\int_{V_j} \Sigma_T^0(\bar{r},E)\phi(\bar{r},E)dV = \sum_a \int_{S_a} \Psi_{in}(\bar{r}',\bar{\Omega},E) \int_{V_j} \Sigma_T^0(\bar{r},E) \frac{\exp\Big[-\tau(\bar{r}',\bar{r},E)\Big]}{\|\bar{r}-\bar{r}'\|^2} dS' \big|\bar{\Omega}\cdot\bar{n}\big| dV + \sum_i \int_{V_i} q(\bar{r}',\bar{\Omega},E) \int_{V_j} \Sigma_T^0(\bar{r},E) \frac{\exp\Big[-\tau(\bar{r}',\bar{r},E)\Big]}{\|\bar{r}-\bar{r}'\|^2} dV'dV \tag{25}$$

If a isotropic emission density is assumed:

$$\int_{V_j} \Sigma_T^0(\bar{r},E)\phi(\bar{r},E)dV = \sum_a \int_{S_a} \Psi_{in}(\bar{r}',\bar{\Omega},E) \int_{V_j} \Sigma_T^0(\bar{r},E) \frac{\exp\Big[-\tau(\bar{r}',\bar{r},E)\Big]}{\|\bar{r}-\bar{r}'\|^2} dS' \big|\bar{\Omega}\cdot\bar{n}\big| dV + \sum_i \int_{V_i} Q(\bar{r}',\bar{\Omega},E) \int_{V_j} \Sigma_T^0(\bar{r},E) \frac{\exp\Big[-\tau(\bar{r}',\bar{r},E)\Big]}{\|\bar{r}-\bar{r}'\|^2} dV'dV \tag{26}$$

Equation 26 may be rewritten in a more compact form as:

$$\Sigma_{T,j}^0(E)\phi_j(E)V_j = \sum_a S_a J_{in,a}(E) P_{a\to j}(E) + \sum_i V_i Q_i(E) P_{i\to j}(E) \tag{27}$$

This equation represents the local problem and will be used to calculate the neutron flux inside each region of the system. The probabilities in equation 27 are:

- $P_{g,i\to j}$ - the probability for a neutron of energy group g, emitted isotropically in volume V_i, with a given emission density, to have its first collision in volume V_j.
- $P_{g,a\to j}$ - the probability for a neutron of energy group g, entering through surface a, to have its first collision in volume V_i.

The first term on the right hand side (RH) will be the contribution of incoming neutron currents to the neutron flux in region j and the second term will be the contribution of neutrons emitted in region i going to region j.

2.1.2 Global problem

If equation 16 is written for the outgoing angular flux instead, we get:

$$\begin{aligned}\Psi(\bar{r}_{out},\bar{\Omega},E) = \\ \Psi(r_{in},\bar{\Omega},E)\cdot\exp\Big[-\tau(\bar{r}_{in},\bar{r}_{out},E)\Big]+ \\ +\int_{s_{in}}^{0} q(\bar{r}_{out}-\bar{s}\bar{\Omega},\bar{\Omega},E)\cdot\exp\Big[-\tau(\bar{r}',\bar{r}_{out},E)\Big]ds'\end{aligned} \tag{28}$$

If equation 28 is multiplied by $\left|\bar{\Omega}\cdot\bar{n}\right|$ and integrating on a a given surface S and for solid angles such that $\left|\bar{\Omega}\cdot\bar{n}\right|>0$ gives:

$$\begin{aligned}\int_S\int_{2\pi,\bar{\Omega}\cdot\bar{n}>0}\Psi(\bar{r}_{out},\bar{\Omega},E)\left|\bar{\Omega}\cdot\bar{n}\right|dSd\omega = \\ \int_S\int_{2\pi,\bar{\Omega}\cdot\bar{n}>0}\Psi(r_{in},\bar{\Omega},E)\cdot\exp\Big[-\tau(\bar{r}_{in},\bar{r},E)\Big]\left|\bar{\Omega}\cdot\bar{n}\right|dSd\omega+ \\ +\int_S\int_{2\pi,\bar{\Omega}\cdot\bar{n}>0}\left|\bar{\Omega}\cdot\bar{n}\right|\int_{s_{in}}^{0} q(\bar{r}-\bar{s}'\bar{\Omega},\bar{\Omega},E)\cdot\exp\Big[-\tau(\bar{r}',\bar{r},E)\Big]ds'dSd\omega\end{aligned} \tag{29}$$

At the interface defined by $\bar{r}_{in}=\bar{r}-s_{in}\bar{\Omega}$ the infinitesimal surface element spanned by a change of the direction $\bar{\Omega}$ is given by:

$$dS\left|\bar{\Omega}\cdot\bar{n}\right| = s_{in}^2 d\omega = \|\bar{r}-\bar{r}_{in}\|d\omega \tag{30}$$

At the point defined by: $\bar{r}'=\bar{r}-s\bar{\Omega}$ the infinitesimal volume element spanned by a change of direction $\bar{\Omega}$ and the abscissa s' is given by:

$$dV' = s'^2 ds' d\omega = \left\|\bar{r}-\bar{r}'\right\|ds'd\omega \tag{31}$$

Using equation 30 and 31 in equation 29 allows for replacing the first solid angle integral with a surface integral and the second double integral on all solid angles and the abscissa s by a volume integral. This gives:

$$\begin{aligned}\int_S\int_{2\pi,\bar{\Omega}\cdot\bar{n}>0}\Psi(\bar{r},\bar{\Omega},E)\left|\bar{\Omega}\cdot\bar{n}\right|dSd\omega = \\ \int_S\left|\bar{\Omega}\cdot\bar{n}\right|dS\int_S\Psi(\bar{r}',\bar{\Omega}_m,E)\cdot\frac{\exp\Big[-\tau(\bar{r}',\bar{r},E)\Big]}{\|\bar{r}-\bar{r}'\|}\left|\bar{\Omega}\cdot\bar{n}\right|dS'+ \\ +\int_S\left|\bar{\Omega}\cdot\bar{n}\right|dS\int_V q(\bar{r}',\bar{\Omega},E)\cdot\frac{\exp\Big[-\tau(\bar{r}',\bar{r},E)\Big]}{\|\bar{r}-\bar{r}'\|}dV'\end{aligned} \tag{32}$$

As before the volume V of the system may be partitioned into sub-volumes V_i, such that $V=\bigcup_i V_i$, and the outer surface S may be partitioned into sub-surfaces S_a, such that $S=\bigcup_a S_a$:

$$\begin{aligned}\int_{S_a}\int_{2\pi,\bar{\Omega}\cdot\bar{n}>0}\Psi(\bar{r},\bar{\Omega},E)\big|\bar{\Omega}\cdot\bar{n}\big|dSd\omega = \\ \sum_b\int_{S_a}\big|\bar{\Omega}\cdot\bar{n}\big|dS\int_{S_b}\Psi(\bar{r}',\bar{\Omega},E)\cdot\frac{\exp\Big[-\tau(\bar{r}',\bar{r},E)\Big]}{\|\bar{r}-\bar{r}'\|}\big|\bar{\Omega}\cdot\bar{n}\big|dS'+ \\ +\sum_i\int_{S_a}\big|\bar{\Omega}\cdot\bar{n}\big|dS\int_{V_i}q(\bar{r}',\bar{\Omega},E)\cdot\frac{\exp\Big[-\tau(\bar{r}',\bar{r}_{out},E)\Big]}{\|\bar{r}-\bar{r}'\|}dV'\end{aligned} \tag{33}$$

If isotropic emission density is assumed once again:

$$\begin{aligned}\int_{S_a}\int_{2\pi,\bar{\Omega}\cdot\bar{n}>0}\Psi(\bar{r},\bar{\Omega},E)\big|\bar{\Omega}\cdot\bar{n}\big|dSd\omega = \\ \sum_b\int_{S_a}\big|\bar{\Omega}\cdot\bar{n}\big|dS\int_{S_b}\Psi(\bar{r}',\bar{\Omega},E)\cdot\frac{\exp\Big[-\tau(\bar{r}',\bar{r},E)\Big]}{\|\bar{r}-\bar{r}'\|}\big|\bar{\Omega}\cdot\bar{n}\big|dS'+ \\ +\sum_i\int_{S_a}\big|\bar{\Omega}\cdot\bar{n}\big|dS\int_{V_i}Q(\bar{r}',E)\cdot\frac{\exp\Big[-\tau(\bar{r}',\bar{r}_{out},E)\Big]}{4\pi\|\bar{r}-\bar{r}'\|}dV'\end{aligned} \tag{34}$$

The solid angle-integrated emission density Q will be given by:

$$Q(\bar{r}',E)=\int_0^\infty\Big[\Sigma_{s0}^0(\bar{r}',E'\to E)+\frac{\chi(E)}{k}\nu(E')\Sigma_f(E')\Big]\phi(\bar{r}',E')dE' \tag{35}$$

As before equation 34 may be rewritten in a more compact form:

$$S_aJ_{out,a}(E)=\sum_b S_bJ_{in,b}(E)P_{b\to a}(E)+\sum_i V_iQ_i(E)P_{i\to a}(E) \tag{36}$$

Equation 36 is the global problem and may be used to calculate the neutron currents into each sub-system. The probabilities used in this equations are:

- $P_{b\to a}$: the probability for a neutron of energy group g, entering through surface b, to leave through surface a without any interaction inside the system.
- $P_{i\to a}$: the probability for a neutron of energy group g, emitted isotropically in volume V_i, with a given emission density, to leave the system through surface a.

The first term on the RH will give the contribution to the neutron currents out due to the neutron currents in through the other surfaces. The second term will give the contribution from neutrons emitted in a region to the neutron current out through a surface.

2.2 Response matrix formulation

If the system contains $I = 1...N$ subsystems having volumes V_i and surfaces S_i equations 27 and 36 may be written for each subsystem, with multi-group formalism introduced, as:

$$\Sigma^0_{T,j,g}\phi_{j,g}V_j = \sum_{a\in S_i} S_a J_{in,a,g} P_{a\to j,g} + \sum_{i\in V_i} V_i Q_{i,g} P_{i\to j,g} \tag{37}$$

$$S_a J_{out,a,g} = \sum_{b\in S_i} S_b J_{in,b,g} P_{b\to a,g} + \sum_{i\in V_i} V_i Q_{i,g} P_{i\to a,g} \tag{38}$$

Equation 37 may be cast into matrix form as:

$$\bar{J}^I_{out} = \bar{\bar{R}}^I \times \bar{J}^I_{in} + \bar{J}^I_{source} \tag{39}$$

The matrix $\bar{\bar{R}}^I$ is the response matrix for the subsystem I. This equation may be written for any subsystem and hence it may be given as:

$$\bar{J}_{out} = \bar{\bar{R}} \times \bar{J}_{in} + \bar{J}_{source} \tag{40}$$

Here $\bar{\bar{R}}$ will be the response matrix for the whole system. The structure and the construction of the $\bar{\bar{R}}$ matrix will be discussed later.

Since a topographical relationship exists between the outgoing current from a given subsystem to the incoming current of its neighbouring subsystem:

$$\bar{J}_{in} = \bar{\bar{P}} \times \bar{J}_{out} \tag{41}$$

If equation 40 and 41 are combined the global problem may be determined:

$$\bar{J}_{in} = \bar{\bar{P}} \times \bar{\bar{R}} \times \bar{J}_{in} + \bar{\bar{P}} \times \bar{J}_{source} \tag{42}$$

Equation 40 may also be cast into a matrix equation as:

$$\bar{\phi}^I = \bar{\bar{S}} \times \bar{J}_{in} + \phi^I_{source} \tag{43}$$

which will define the local problem.

2.3 Power iteration method

In order to update the multiplication factor k the power iteration method is used. The multigroup transport equation may be recast on a generic matrix form as:

$$\bar{\bar{L}} \times \bar{\Psi} = (\bar{\bar{H}} + \frac{1}{k}\bar{\bar{F}})\bar{\Psi} \tag{44}$$

where the flux vector is a column vector with fluxes for all regions and groups for length. The L matrix is a transport matrix that relates the angular flux to the source terms of scattering and fission. The H and F matrices are for scattering and fission respectively. The effective multiplication factor may be updated by rewriting equation 44 as:

$$(\bar{\bar{L}} - \bar{\bar{H}}) \times \bar{\Psi} = \frac{1}{k}\bar{\bar{F}} \times \bar{\Psi} \tag{45}$$

It can be noted that the fission operator acts upon the angular flux integrated on all angles and hence may be replaced by:

$$\bar{\bar{F}} \times \bar{\Psi} = \bar{\bar{F}}_\phi \times \bar{\phi} \tag{46}$$

A matrix M may be defined as:

$$\bar{\bar{M}} = \bar{\bar{L}} - \bar{\bar{H}} \tag{47}$$

and hence equation 45 may be rewritten as:

$$\bar{\bar{M}} \times \bar{\Psi} = \frac{1}{k}\bar{\bar{F}}_\phi \times \bar{\phi} \tag{48}$$

or alternatively as:

$$\bar{\Psi} = \frac{1}{k}\bar{\bar{M}}^{-1} \times \bar{\bar{F}}_\phi \times \bar{\phi} \tag{49}$$

Assuming that the iteration has converged the angular flux at an iteration p is given by:

$$\bar{\Psi}^{(p)} = \frac{1}{k^{(p-1)}}\bar{\bar{M}}^{-1} \times \bar{\bar{F}}_\phi \times \bar{\phi}^{(p-1)} \tag{50}$$

The angular flux may be rewritten as before as:

$$\Psi^{(p)} = \bar{\bar{F}}_\phi \times \bar{\phi}^{(p)} \tag{51}$$

giving:

$$\bar{\bar{F}}_\phi \times \bar{\phi}^{(p)} = \frac{1}{k^{(p-1)}} \bar{\bar{F}} \times \bar{\bar{M}}^{-1} \times \bar{\bar{F}}_\phi \times \bar{\phi}^{(p-1)} \tag{52}$$

Introducing the matrix $\bar{\bar{A}} = \bar{\bar{F}} \times \bar{\bar{M}}^{-1}$ and the vector $\bar{x} = \bar{\bar{F}}_\phi \times \bar{\phi}$ equation 52 may be simplified as:

$$\bar{x}^{(p)} = \frac{1}{k^{(p-1)}} \bar{\bar{A}} \times \bar{x}^{(p-1)} \tag{53}$$

When the iteration has converged, equation 53 may be rewritten as:

$$\bar{x}^{(\infty)} = \frac{1}{k^{(\infty)}} \bar{\bar{A}} \times \bar{x}^{(\infty)} \tag{54}$$

Rewriting equation 54 the effective multiplication factor may be expressed as:

$$k^{(\infty)} = \frac{\bar{x}^{(\infty)} \cdot \bar{\bar{A}} \times \bar{x}^{(\infty)}}{\bar{x}^{(\infty)} \cdot \bar{x}^{(\infty)}} \tag{55}$$

This expression may be used to determine the new effective multiplication factor once $\bar{x}$ has been determined by:

$$k^{(p)} = \frac{\bar{x}^{(p-1)} \cdot \bar{\bar{A}} \times \bar{x}^{(p-1)}}{\bar{x}^{(p-1)} \cdot \bar{x}^{(p-1)}} \tag{56}$$

Using equation 56 and 53 the following equation is obtained:

$$k^{(p)} = k^{(p-1)} \times \frac{\bar{x}^{(p-1)} \cdot \bar{x}^{(p)}}{\bar{x}^{(p-1)} \cdot \bar{x}^{(p-1)}} \tag{57}$$

The iterative solution shown above is the power iteration method and will converge to the largest k eigenvalue, the interested reader can find proof for this in literature [8].

The set of equations used in the response matrix formulation, the global and local problem, need to be recast into a form that corresponds to the generic matrix formulation given by equation 44. In this case the global problem is used. Taking the converged global balance equation:

$$\Sigma^0_{T,j,g} \phi_{j,g} V_j = \sum_{a \in S_i} S_a J_{in,a,g} P_{a \to j,g} + \sum_{i \in V_i} V_i Q_{i,g} P_{i \to j,g} \tag{58}$$

and expressing it in the form of the generic transport equation:

$$\Sigma^0_{T,j,g} \phi_{j,g} V_j - \sum_{a \in S_i} S_a J_{in,a,g} P_{a \to j,g} - \sum_{i \in V_i} V_i Q^{scattering}_{i,g} P_{i \to j,g} = \sum_{i \in V_i} V_i Q^{fission}_{i,g} P_{i \to j,g} \tag{59}$$

The right-hand side of equation 59 will give the x vector given by $\bar{x} = \bar{\bar{F}} \times \bar{\phi}$. The specific contributions to each part of the x vector may be given by:

$$x_{g,j} = \sum_{i \in V_i} V_i Q_{g,i}^{fission} P_{g,i \to j} = \sum_{i \in V_i} V_i P_{g,i \to j} \chi_{g,i} \sum_{g'} (\nu \Sigma_f)_{g',i} \phi_{g',i} \tag{60}$$

It may be seen from equation 60 that the components needed to build the fission matrix F will be contained in this equation.

3 System

In this section the system that is modelled will be described with all important parameters specified.

3.1 Assembly system

In this project a simplified boiling water reactor (BWR) fuel assembly will be modelled. The fuel assembly specification was found on the Serpent Wiki homepage in their collection of example input files [9]. The original example file featured a 2D asymmetric BWR assembly with Gd-pins. It had a 10x10 fuel lattice with a water channel asymmerically placed in the assembly. The initial fuel assembly geometry may be seen in figure 2.

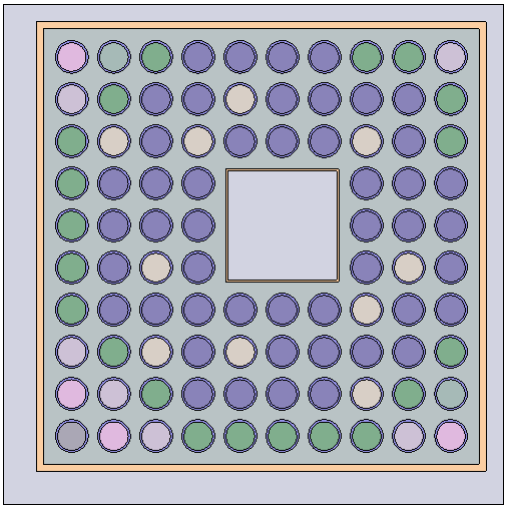


Figure 2: Original 2D assymetrical fuel assembly with water channel.

The specific parameters for the modelled geometry may be found in table 1 below:

Table 1: Important parameters for the 2D fuel assembly.

Parameter	Data
Pin pitch	1.295 cm
Assembly pitch	15.375 cm
Outer water channel half-width	1.7445 cm
Inner water channel half-width	1.6742 cm

Modelling the fuel assembly as a whole in Serpent would not pose a problem, however, when calculating the probabilities in Serpent the addition of a water channel would complicate the calculations and hence the water hole is removed to make the system as simple as possible in the development stages of the method. Further the water gaps between each assembly were also removed. The new simplified system is show in figure 3 below:

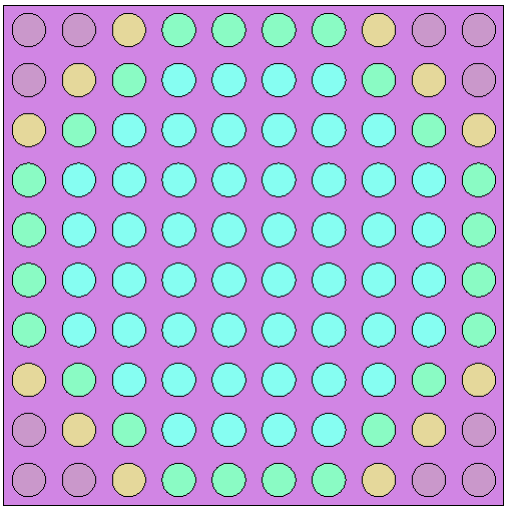


Figure 3: Simplified 2D asymmetrical fuel assembly with a symmetrical fuel pin placement.

In figure 3 the different colours for each fuel pin indicates the fuel pin enrichment. The fuel assembly has to following pin configuration:

$$\begin{bmatrix} 2 & 2 & 3 & 5 & 5 & 5 & 5 & 3 & 2 & 2 \\ 2 & 3 & 5 & 6 & 6 & 6 & 6 & 5 & 3 & 2 \\ 3 & 5 & 6 & 6 & 6 & 6 & 6 & 6 & 5 & 3 \\ 5 & 6 & 6 & 6 & 6 & 6 & 6 & 6 & 6 & 5 \\ 5 & 6 & 6 & 6 & 6 & 6 & 6 & 6 & 6 & 5 \\ 5 & 6 & 6 & 6 & 6 & 6 & 6 & 6 & 6 & 5 \\ 5 & 6 & 6 & 6 & 6 & 6 & 6 & 6 & 6 & 5 \\ 3 & 5 & 6 & 6 & 6 & 6 & 6 & 6 & 5 & 3 \\ 2 & 3 & 5 & 6 & 6 & 6 & 6 & 5 & 3 & 2 \\ 2 & 2 & 3 & 5 & 5 & 5 & 5 & 3 & 2 & 2 \end{bmatrix}$$

where the enrichment of each pin is specified in the next section.

3.2 Fuel pin system

The probabilities needed for the response matrix formulation need to be determined for each fuel pin. In total there are six fuel pins with different enrichment as well as a seventh fuel pin containing Gd. The modelled fuel pin system is a simple fuel rod (without cladding or gap) surrounded by moderator. The fuel pin system can be seen in figure 4 below:

The important parameters for the fuel cell system can be seen in table 2 below:

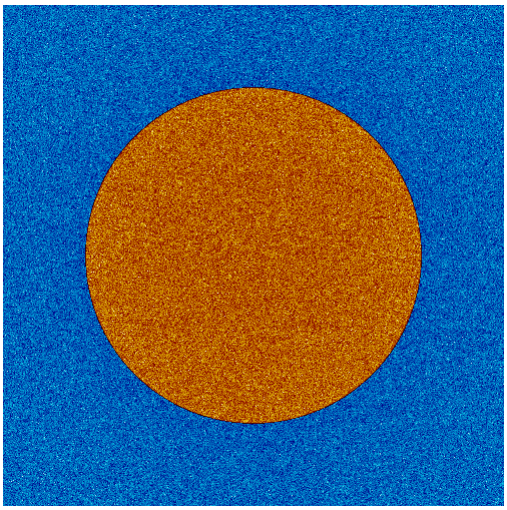


Figure 4: Fuel pin system, simplified fuel cell without cladding or gap.

Table 2: Important parameters for the fuel cell system.

Parameter	Data
Pin pitch	1.295 cm
Fuel radius	0.4335 cm

The fuel compositions are given in table 3 below:

Table 3: Mass fractions of each material present in the fuel.

Fuel pin number	U-235	U-238	O-16
1	0.015867	0.86563	0.1185
2	0.018512	0.86299	0.1185
3	0.022919	0.85858	0.1185
4	0.026445	0.85505	0.1185
5	0.029971	0.85153	0.1185
6	0.032615	0.84888	0.1185

The material composition of the Gd pin is defined in table 4 below:

Table 4: Material composition of fuel pin 7, the Gd pin.

Material	Mass composition
U-235	0.0313109
U-238	0.814929
Gd-152	6.70544E-05
Gd-154	7.13344E-04
Gd-155	5.06012E-03
Gd-156	7.08860E-03
Gd-157	5.43718E-03
Gd-158	8.64341E-03
Gd-160	7.69426E-03
O-16	0.019056

4 Implementation

The implementation procedure of the code is described in this section.

4.1 Calculating probabilities in Serpent2

As mentioned in the theory there are four probabilities that need to be determined for each subsystem. These are:

- $P_{g,i\to j}$ - the probability for a neutron of energy group g, emitted isotropically in volume V_i, with a given emission density, to have its first collision in volume V_j.
- $P_{g,i\to a_i}$ - the probability for a neutron of energy group g, emitted isotropically in volume V_i, with a given emission density, to escape the system without interaction through surface a_i.
- $P_{g,a\to i}$ - the probability for a neutron of energy group g, entering through surface a, to have its first collision in volume V_i.
- $P_{g,a\to b}$ - the probability for a neutron of energy group g, entering through surface a, to leave through surface b without interacting with the system.

In Serpent2 these probabilities will be calculated using detectors, surface and material, in combination with a newly introduced flagging feature. A surface detector is specified as:

```
det <detector name> ds <surface name> <direction>
```

The direction is defined differently depending on whether it is a plane surface or a surface of a geometry and is defined by a -1 or 1. For a plane the direction is specified by the positive direction of the positive coordinate axis and for a geometry surface the inward directions is defined as -1 and outward direction as 1.

The flagging feature allows for setting and removing flags if a detector is scored and scoring a detector if a flag is or is not set [10]. The flagging feature, called "dfl" has two inputs and is written as follows:

```
dfl <flag number> <option>
```

Where the flag number is the number associated with a certain flag and the option has four different inputs from 0 to 3:

- 0: remove the specified flag number when the detector is scored.
- 1: set the specified flag number when the detector is scored.
- -2/2: check if the specified flag number is set and score detector if set.
- -3/3: check if the specified flag number is set and score detector if <u>not</u> set.

Further there is an option to set whether a series of "dfl" tests act on an "or" or an "and" logic. This is done by setting a minus sign in front of the $<$ *option* $>$.

By the definition of probabilities a set of probabilities must add up to unity and hence sets of probabilities may be found from the four probabilities that can be calculated together.

4.1.1 Neutrons entering through a surface

The first set of probabilities are those due to a neutron entering the system through a surface. If looking at a specific surface a, any neutron entering through this surface must either leave the system again, through another surface, or react within the system, through scattering or absorption:

$$J_{in,a} = R_{moderator} + R_{fuel} + J_{out,2} + J_{out,3} + J_{out,4} \tag{61}$$

Normalising equation 61 with the current in through surface a the equation may be rewritten as:

$$\sum_{b \in S_I} P_{g,a \to b} + \sum_{i \in V_i} P_{g,a \to i} = 1 \tag{62}$$

This set of probabilities may be calculated by using a surface detector on one surface of the system, that measures the current of neutrons into the system, and setting flag 1 when this detector is scored.

```
det surface_A ds A 1 dfl 1 2
```

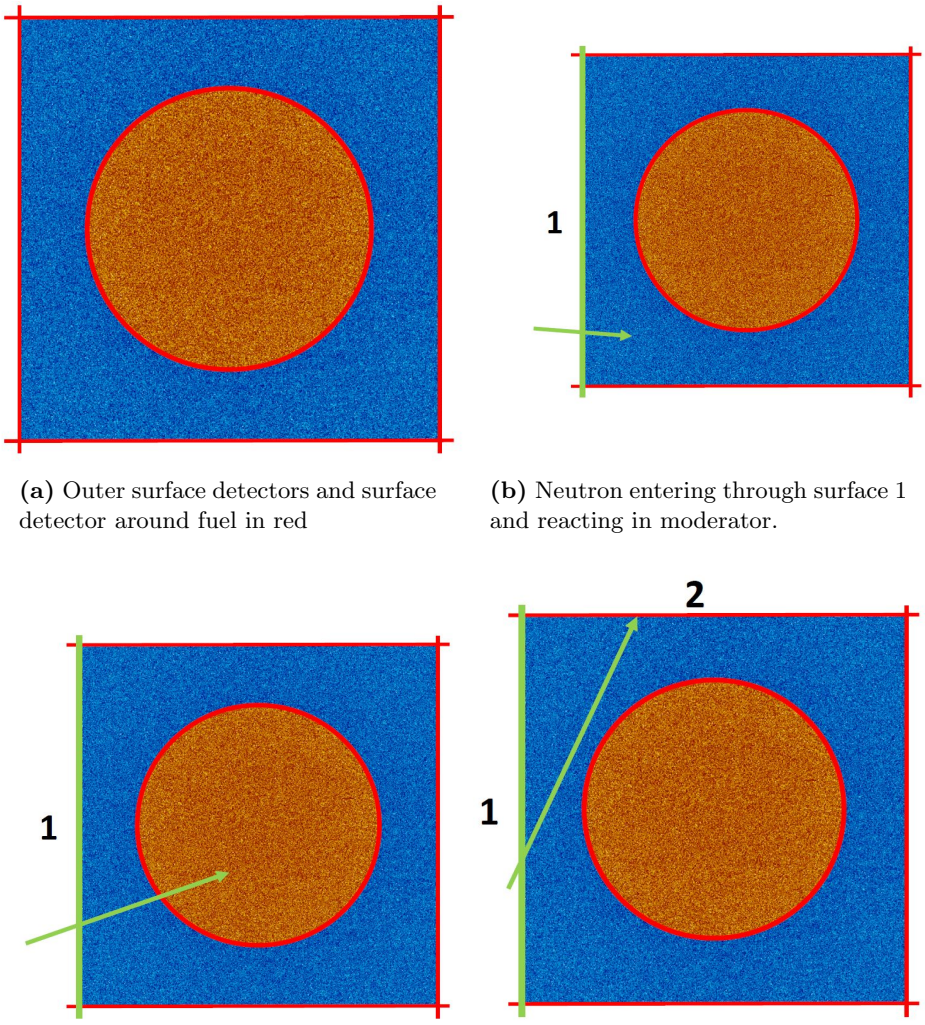
This will calculate all neutrons entering the system through the west surface and will also be used as the normalisation to calculate the probabilities. The surface detectors can be seen in figure 5a. Two material detectors are used in the moderator and fuel, with the criteria that flag 1 is set, to count all neutrons that have entered through the west surface that reacts in fuel and moderator. These also have the dfl setting that when the detector is scored flag 1 is removed, since after interacting with the system the neutron will be treated as coming from that region rather than from the west surface. These detectors may be seen in figures 5c and 5b.

```
det fuel_interaction dm fuel1 dr -1 fuel1 dfl 1 2 dfl 1 0
det moderator_interaction dm cool dr -1 cool dfl 1 2 dfl 1 0
```

Another four surface detectors are used to calculate the current out of the system with the criteria that 1 flag is set. This will give the contribution from the west surface since any neutron that has interacted with the system will lead to removal of flag 1 and hence would not be counted. The contributions may be seen in figure 5d The three surface detectors are defined as:

```
det surface_east ds east 1 dfl 1 2 dfl 1 0
det surface_south ds south -1 dfl 1 2 dfl 1 0
det surface_north ds north 1 dfl 1 2 dfl 1 0
```

It is not necessary to measure the neutron current out through the west surface since only neutrons that have not interacted with the system are counted and it is impossible for a neutron to enter and leave through the same surface without interacting with the system.



(a) Outer surface detectors and surface detector around fuel in red

(b) Neutron entering through surface 1 and reacting in moderator.

(c) Neutron entering through surface 1 and reacting in fuel

(d) Neutron entering through surface 1 and leaving through surface 2.

Figure 5: The different neutron paths for a neutron entering through a surface.

4.1.2 Neutrons emitted from a region

Similarly two more sets of probabilities may be defined for neutrons being emitted from a region in the system. Since there are two regions, fuel and moderator, there will be two sets of probabilities that need to be calculated in serpent.

$$Emitted_{fuel} = R_{fuel} + R_{moderator} + J_{out,1} + J_{out,2} + J_{out,3} + J_{out,4} \tag{63}$$

$$Emitted_{moderator} = R_{moderator} + R_{fuel} + J_{out,1} + J_{out,2} + J_{out,3} + J_{out,4} \tag{64}$$

Both equations 63 and 64 may be normalised by the total number of neutrons emitted:

$$\sum_{a \in S_I} P_{g,fuel \to a} + \sum_{i \in V_i} P_{g,fuel \to i} = 1 \tag{65}$$

$$\sum_{a \in S_I} P_{g,moderator \to a} + \sum_{i \in V_i} P_{g,moderator \to i} = 1 \tag{66}$$

The two sums of probabilities are for neutrons emitted from a region i to leave to a surface or react in a region inside the system respectively. Calculating these sets of probabilities is more complicated than the previous set of probabilities due to two complications that both are directly related to the calculation of neutrons emitted in one region to have their first collision in the same region.

The first complication is for determining which neutrons have been emitted from the region. The dfl flagging feature does not allow for flagging source neutrons. This problem was remedied by adding a line of code to the source code in Serpent that automatically flagged any source neutrons with flag number 1. Hence calculating the number of neutrons emitted in a region and having their first interaction in the same region was simply calculated by checking all reactions in the material while flag 1 was set.

The second complication was the calculation of neutrons scattering in a region and then interacting in the same region. This is treated as an emitted neutron in the response matrix method and hence needs to be determined. The problem in this case is due to Serpent not being able to distinguish between a first scattering interaction and a second. To measure the second scattering interaction in a material a flag would have to be set for the first scattering interaction. However, when detecting a first scattering interaction the second would be scored as well since the scattering happens in the same neutron history. This problem was solved by calculating the scattering within one region from equation 65 or 66 since all other terms in these equations may be determined in Serpent.

The calculation of all the contributions needed for the sets of equations 65 and 66 is more complex and a large number of detectors are needed with intricate dfl flagging compositions. The different steps made in the calculation of the probabilities and the associated detectors needed are shown in the table below:

Table 5: Detectors used to determine basic contributions.

Contribution calculated	Detector	Flag set	Criteria
Scattering in fuel	material	11	Flag 1 not set
Scattering in moderator	material	12	Flag 1 not set
Fuel to moderator	material	-	Flag 11 set
Fuel to surface	surface	-	Flag 11 set
Moderator to fuel	material	-	Flag 12 set
Moderator to surface	surface	-	Flag 12 set
Source to fuel	material	-	Flag 1 set
Source to moderator	material	-	Flag 1 set
Source to surface	surface	-	Flag 1 set
Surface in	surface	Surface flag (1,2,3,4)	-
Surface to moderator	material	-	Surface flag set
Surface to fuel	material	-	Surface flag set

These calculations are done for thermal and fast neutrons. Further one also needs to take into consideration neutrons that change energy group and that may change both energy group and region. These contributions are calculated using the detectors shown in table 6 below:

Table 6: Detectors used to determine energy group change contributions.

Contribution calculated	Detector	Flag set	Criteria
Fast scattering fuel	material	50	-
Fast scattering moderator	material	51	-
Thermal scattering fuel	material	52	-
Thermal scattering moderator	material	53	-
Fuel to moderator, fast to thermal	material	-	Flag 50 set
Moderator to fuel, fast to thermal	material	-	Flag 51 set
Fuel to fuel, fast to thermal	material	-	Flag 50 set
Moderator to moderator, fast to thermal	material	-	Flag 51 set
Fuel to moderator, thermal to fast	material	-	Flag 52 set
Moderator to fuel, thermal to fast	material	-	Flag 53 set
Fuel to fuel, thermal to fast	material	-	Flag 52 set
Moderator to moderator, thermal to fast	material	-	Flag 53 set

The detectors used to calculate the energy group change also use the Serpent detector energy bin setting *de* that can set the energy range in which neutrons are counted. A typical detector would look as follows:

```
det fuelmod_12 dm cool dr -1 cool de 2gthm dfl 50 2 dfl 50 0
```

This detector would calculate neutrons going from fuel to moderator, from fast to thermal energy group. The energy bin where neutrons are counted is the thermal bin because of the dfl criteria stating that flag 50 has to be set (where flag 50 is set when a fast neutron is scattered) the neutrons counted would only be thermal neutrons that were fast before scattering. As seen in table 6 eighth of these detectors are needed to measure all regions and energy groups.

In order to determine the contribution from scattering from one region to itself it is needed to determine all contributions that could lead to a scattering interaction in that region. If all contributions but one, to the reaction rate in the region, are known, the last contribution may be determined according to:

$$R_{g,i\to i} = R_{g,tot\,i} - R_{source\to i} - R_{j\to i} - 4 \times R_{surface\to i} - \\ - R_{j\to i,g'\to g} - R_{i\to i,g'\to g} \tag{67}$$

Equation 67 may be normalised by the total reaction rate and the probability for scattering from a region to itself may be calculated by:

$$P_{g,i\to i} = \frac{R_{g,tot\,i} - R_{source\to i} - R_{j\to i} - 4 \times R_{surface\to i}}{R_{g,tot\,i}} - \\ - \frac{R_{j\to i,g'\to g} - R_{i\to i,g'\to g}}{R_{g,tot\,i}} \tag{68}$$

This is done for both regions, fuel and moderator, and both energy groups, thermal and fast.

4.2 Labelling the system

The simplest system that can be set up is a 2x2 system of pin cells. The labelling of the system is important in order to keep track of all currents, to know the material of the regions and to have the correct format of the matrices used.

The first step is to label all cells in the system. The labelling of a simple 2x2 system would look as follows:

1	3
2	4

and the motivation to label the cells in this order is that the index of a matrix are numbered in the same order and hence the cells can be accessed using only one index. The surfaces are numbered continuously in order of each cell and going clockwise from the west surfaces in each cell. Each cell will have four surfaces belonging to it and in total there will be four times the number of cells surfaces, ie. for a 2x2 system there will be 16 surfaces.

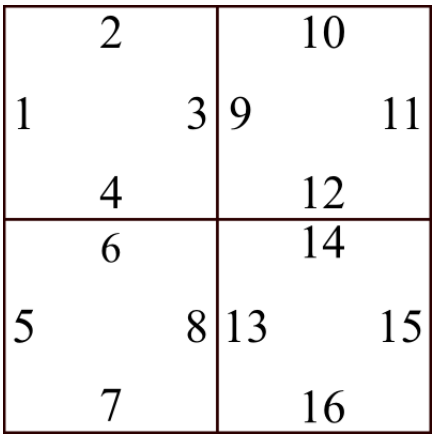


Figure 6: Numbering of surfaces

In each cell there will be a defined number of regions comprised of fuel and moderator. The regions are numbered continuously in order of each cell and going from the centre most region outwards. In the simplest case where there is only one fuel region and one moderator region, the total number of regions is determined as the number of cells times the number of regions, for a 2x2 system there will be eight regions.

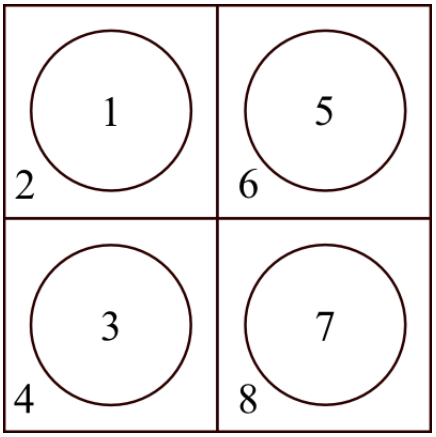


Figure 7: Numbering of regions.

4.3 Structure of deterministic MatLab code

The structure of the code may be seen in figure 8 below:

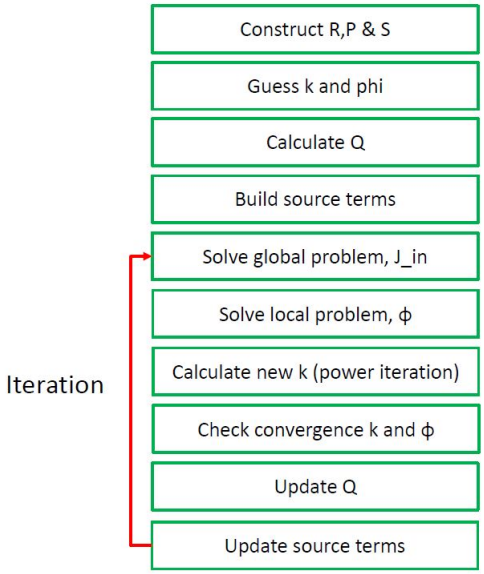


Figure 8: The structure of the MatLab code.

The first step is to construct the response matrix (R), topological matrix (P), local response matrix (S) and fission matrix (F). The matrices only need to be determined once for the system used and may be computed in separate functions. The second step is to make an initial guess for the effective multiplication factor and the scalar neutron flux. This will allow for calculating an initial neutron emission density Q. Using the neutron emission density the source terms can be calculated as well as the source current and the source flux that are used in the global and local problem respectively.

The first step in the iteration is to solve the global problem to determine the currents into the system, J_{in} according to:

$$\bar{J}_{in} = \bar{\bar{P}} \times \bar{\bar{R}} \times \bar{J_{in}} + \bar{\bar{P}} \times \bar{J}_{source}$$

Next the local problem may be solved using J_{in} to give the neutron flux, ϕ:

$$\phi = \bar{S} \times \bar{J_{in}} + \phi_{source}$$

Using the scalar neutron flux a new effective multiplication factor may be calculated using the power iteration method and the fission matrix F. After a new k has been determined the convergence can be checked with respect to both the scalar neutron flux and the effective multiplication factor. In both cases the relative maximum difference between two iterations

is used as convergence criteria. If the iteration has not converged the emission density may be updated giving new updated source terms and the iteration will continue.

4.4 Building response matrix R

The response matrix $\bar{\bar{R}}$ will relate the outgoing neutron currents in response to the ingoing neutron currents. The response matrix will be a square matrix (n×n) where n will be the total number of ingoing currents. Since the calculations are done with two energy groups there will be a response matrix related to each energy group. The structure of the response matrix may be determined by equation 69.

$$S_a J_{out,g,a} = \sum_{b \in S_i} S_b J_{in,g,b} P_{g,b \to a} + \sum_{i \in V_I} V_i Q_{g,i} P_{g,i \to a} \tag{69}$$

Which in a generic form may be written as:

$$\bar{J}_{in} = \bar{\bar{P}} \times \bar{\bar{R}} \times \bar{J_{in}} + \bar{\bar{P}} \times \bar{J}_{source}$$

It may be seen that the response matrix will be comprised of the ratio between surface b and a times the probability to go from surface b to a. In the case where the surfaces are identical the ratio becomes unity and this term disappears. Since the response matrix will be multiplied by a vector, containing the ingoing currents for each surface, the probabilities of going from surface b to a will need to be placed in the correct positions of the R matrix.

Looking at one single subsystem I and the contribution to one surface, it can be seen that the terms contributing to the response matrix will be determined by:

$$\begin{aligned} S_a J^I_{out,g,a} = {} & S_{b_1} J_{in,g,b_1} P_{g,b_1 \to a} + S_{b_2} J_{in,g,b_2} P_{g,b_2 \to a} + \\ & + S_{b_3} J_{in,g,b_3} P_{g,b_3 \to a} + S_{b_4} J_{in,g,b_4} P_{g,b_4 \to a} \end{aligned} \tag{70}$$

In the case where the surfaces are of same size the surfaces in equation 70 cancel and the equation may be rewritten as:

$$J^I_{out,g,a} = J_{in,g,b_1} P_{g,b_1 \to a} + J_{in,g,b_2} P_{g,b_2 \to a} + J_{in,g,b_3} P_{g,b_3 \to a} + J_{in,g,b_4} P_{g,b_4 \to a} \tag{71}$$

Casting equation 71 into a matrix equation shows the structure of the response matrix for a subsystem I:

$$\begin{bmatrix} J_{out,g,a_1} \\ J_{out,g,a_2} \\ J_{out,g,a_3} \\ J_{out,g,a_4} \end{bmatrix} = \begin{bmatrix} P_{g,1\to1} & P_{g,2\to1} & P_{g,3\to1} & P_{g,4\to1} \\ P_{g,1\to2} & P_{g,2\to2} & P_{g,3\to2} & P_{g,4\to2} \\ P_{g,1\to3} & P_{g,2\to3} & P_{g,3\to3} & P_{g,4\to3} \\ P_{g,1\to4} & P_{g,2\to4} & P_{g,3\to4} & P_{g,4\to4} \end{bmatrix} \times \begin{bmatrix} J_{in,g,b_1} \\ J_{in,g,b_2} \\ J_{in,g,b_3} \\ J_{in,g,b_4} \end{bmatrix} \tag{72}$$

A response matrix may be written for any subsystem and will yield a 4x4 R^I matrix of the form:

$$\bar{\bar{R}}^I = \begin{bmatrix} P^I_{g,1\to1} & P^I_{g,2\to1} & P^I_{g,3\to1} & P^I_{g,4\to1} \\ P^I_{g,1\to2} & P^I_{g,2\to2} & P^I_{g,3\to2} & P^I_{g,4\to2} \\ P^I_{g,1\to3} & P^I_{g,2\to3} & P^I_{g,3\to3} & P^I_{g,4\to3} \\ P^I_{g,1\to4} & P^I_{g,2\to4} & P^I_{g,3\to4} & P^I_{g,4\to4} \end{bmatrix} \tag{73}$$

and since the probability to go from a surface back to the same surface is zero the diagonal of each R^I matrix will be 0 and we finally get:

$$\bar{\bar{R}}^I = \begin{bmatrix} 0 & P^I_{g,2\to1} & P^I_{g,3\to1} & P^I_{g,4\to1} \\ P^I_{g,1\to2} & 0 & P^I_{g,3\to2} & P^I_{g,4\to2} \\ P^I_{g,1\to3} & P^I_{g,2\to3} & 0 & P^I_{g,4\to3} \\ P^I_{g,1\to4} & P^I_{g,2\to4} & P^I_{g,3\to4} & 0 \end{bmatrix} \tag{74}$$

The complete response matrix for the whole system will then be constructed as follows:

$$\bar{\bar{R}} = \begin{bmatrix} R^1 & 0 & 0 \\ 0 & \ddots & 0 \\ 0 & 0 & R^n \end{bmatrix} \tag{75}$$

The complete $\bar{\bar{R}}$ matrix has blocks of each $\bar{\bar{R}}^I$ matrix on the diagonal and the rest are zeros, creating a sparse matrix. Once the probabilities have been determined for each fuel pin type, ie for all possible subsystems, the blocks of $\bar{\bar{R}}^I$ may be placed in the correct position in the $\bar{\bar{R}}$ matrix using the core map specifying the type of fuel pin in each subsystem.

4.5 Building P matrix

In order to relate the incoming neutron currents to the outgoing currents, a topological matrix $\bar{\bar{P}}$ is used, determined by:

$$\bar{J_{in}} = \bar{\bar{P}} \times \bar{J_{out}} \tag{76}$$

The $\bar{\bar{P}}$ matrix will be a square matrix with the same number of rows and columns as there are surface currents. Building the $\bar{\bar{P}}$ matrix is heavily dependent on the labelling of the system since a different labelling procedure will result in a different $\bar{\bar{P}}$ matrix. The $\bar{\bar{P}}$ matrix will also take into account the reflective boundary condition and hence it will be the coupling to the boundary conditions of the computational domain. The format of the $\bar{\bar{P}}$ matrix may be deducted from the labelling of the system that may be seen in figure 6.

At the boundaries of the system $J_{in} = 1 \times J_{out}$ due to the reflective boundary conditions and elsewhere in the system $J_{in} = 1 \times J_{out}$. Hence the P matrix will consist of 0's and 1's. In a 2x2 system the matrix equation 76 will look as follows:

$$\begin{bmatrix} J_{in,1} \\ J_{in,2} \\ J_{in,3} \\ J_{in,4} \\ J_{in,5} \\ J_{in,6} \\ J_{in,7} \\ J_{in,8} \\ J_{in,9} \\ J_{in,10} \\ J_{in,11} \\ J_{in,12} \\ J_{in,13} \\ J_{in,14} \\ J_{in,15} \\ J_{in,16} \end{bmatrix} = \begin{bmatrix} 1 & 0 & 0 & 0 & 0 & 0 & 0 & 0 & 0 & 0 & 0 & 0 & 0 & 0 & 0 & 0 \\ 0 & 1 & 0 & 0 & 0 & 0 & 0 & 0 & 0 & 0 & 0 & 0 & 0 & 0 & 0 & 0 \\ 0 & 0 & 0 & 0 & 0 & 0 & 0 & 0 & 1 & 0 & 0 & 0 & 0 & 0 & 0 & 0 \\ 0 & 0 & 0 & 0 & 0 & 1 & 0 & 0 & 0 & 0 & 0 & 0 & 0 & 0 & 0 & 0 \\ 0 & 0 & 0 & 0 & 1 & 0 & 0 & 0 & 0 & 0 & 0 & 0 & 0 & 0 & 0 & 0 \\ 0 & 0 & 0 & 1 & 0 & 0 & 0 & 0 & 0 & 0 & 0 & 0 & 0 & 0 & 0 & 0 \\ 0 & 0 & 0 & 0 & 0 & 0 & 0 & 0 & 0 & 0 & 0 & 0 & 1 & 0 & 0 & 0 \\ 0 & 0 & 0 & 0 & 0 & 0 & 0 & 1 & 0 & 0 & 0 & 0 & 0 & 0 & 0 & 0 \\ 0 & 0 & 1 & 0 & 0 & 0 & 0 & 0 & 0 & 0 & 0 & 0 & 0 & 0 & 0 & 0 \\ 0 & 0 & 0 & 0 & 0 & 0 & 0 & 0 & 0 & 1 & 0 & 0 & 0 & 0 & 0 & 0 \\ 0 & 0 & 0 & 0 & 0 & 0 & 0 & 0 & 0 & 0 & 1 & 0 & 0 & 0 & 0 & 0 \\ 0 & 0 & 0 & 0 & 0 & 0 & 0 & 0 & 0 & 0 & 0 & 0 & 0 & 1 & 0 & 0 \\ 0 & 0 & 0 & 0 & 0 & 0 & 1 & 0 & 0 & 0 & 0 & 0 & 0 & 0 & 0 & 0 \\ 0 & 0 & 0 & 0 & 0 & 0 & 0 & 0 & 0 & 0 & 0 & 1 & 0 & 0 & 0 & 0 \\ 0 & 0 & 0 & 0 & 0 & 0 & 0 & 0 & 0 & 0 & 0 & 0 & 0 & 0 & 1 & 0 \\ 0 & 0 & 0 & 0 & 0 & 0 & 0 & 0 & 0 & 0 & 0 & 0 & 0 & 0 & 0 & 1 \end{bmatrix} \times \begin{bmatrix} J_{out,1} \\ J_{out,2} \\ J_{out,3} \\ J_{out,4} \\ J_{out,5} \\ J_{out,6} \\ J_{out,7} \\ J_{out,8} \\ J_{out,9} \\ J_{out,10} \\ J_{out,11} \\ J_{out,12} \\ J_{out,13} \\ J_{out,14} \\ J_{out,15} \\ J_{out,16} \end{bmatrix}$$

As seen above the $\bar{\bar{P}}$ matrix is sparse and relatively simple to determine once the labelling of the system has been done. It is important that the $\bar{\bar{P}}$ matrix is constructed correctly since it contains the only connection to the boundary conditions of the system.

4.6 Building the S matrix

The local problem, written for a subsystem I, is determined by the following equation:

$$\bar{\phi}^I = \bar{\bar{S}}^I \times \bar{J}^I_{in} + \bar{\phi}^I_{source} \tag{77}$$

Which, written for any subsystem, may be given explicitly by:

$$\Sigma^0_{T,g,j}\phi_{g,j}V_j = \sum_{a \in S_i} S_a J_{in,g,a} P_{g,a \to j} + \sum_{i \in V_i} V_i Q_{g,i} P_{g,i \to j} \tag{78}$$

This shows that the structure of the $\bar{\bar{S}}$ matrix, for one region, may be determined from:

$$\phi_{1,g} = \frac{S_1 P_{g,1\to1}}{\Sigma_{T,g,1} V_1} \cdot J_{in,g,1} + \frac{S_2 P_{g,2\to1}}{\Sigma_{T,g,1} V_1} \cdot J_{in,g,2} + \frac{S_1 P_{g,3\to1}}{\Sigma_{T,g,1} V_1} \cdot J_{in,g,3} + \frac{S_1 P_{g,4\to1}}{\Sigma_{T,g,1} V_1} \cdot J_{in,g,4} \quad (79)$$

The flux in the second region of the same cell will be calculated using a similar equation as the one above, however, with different probabilities, total cross-section and volume. If the surface currents are in a column vector the $\bar{\bar{S}}^I$ matrix will have dimensions 2x4 since a single cell has two regions associated with the same four surface currents. Recasting equation 79 into a matrix equation it may be seen that the flux in one region may be calculated by:

$$\begin{bmatrix}\phi_{1,g}\end{bmatrix} = \begin{bmatrix} \frac{S_1 P_{g,1\to1}}{\Sigma_{T,g,1} V_1} & \frac{S_2 P_{g,2\to1}}{\Sigma_{T,g,1} V_1} & \frac{S_3 P_{g,3\to1}}{\Sigma_{T,g,1} V_1} & \frac{S_4 P_{g,4\to1}}{\Sigma_{T,g,1} V_1} \end{bmatrix} \times \begin{bmatrix} J_{in,1} \\ J_{in,2} \\ J_{in,3} \\ J_{in,4} \end{bmatrix} \quad (80)$$

Equation 80 may be written for the second region in the cell as well and combining these two equations a matrix equation may be created with the following structure:

$$\begin{bmatrix}\phi_{1,g} \\ \phi_{2,g}\end{bmatrix} = \begin{bmatrix} \frac{S_1 P_{g,1\to1}}{\Sigma_{T,g,1} V_1} & \frac{S_2 P_{g,2\to1}}{\Sigma_{T,g,1} V_1} & \frac{S_3 P_{g,3\to1}}{\Sigma_{T,g,1} V_1} & \frac{S_4 P_{g,4\to1}}{\Sigma_{T,g,1} V_1} \\ \frac{S_1 P_{g,1\to2}}{\Sigma_{T,g,2} V_2} & \frac{S_2 P_{g,2\to2}}{\Sigma_{T,g,2} V_2} & \frac{S_3 P_{g,3\to2}}{\Sigma_{T,g,2} V_2} & \frac{S_4 P_{g,4\to2}}{\Sigma_{T,g,2} V_2} \end{bmatrix} \times \begin{bmatrix} J_{in,1} \\ J_{in,2} \\ J_{in,3} \\ J_{in,4} \end{bmatrix} \quad (81)$$

From which it may be seen that the $\bar{\bar{S}}^I$ matrix will be given by:

$$\bar{\bar{S}}^I = \begin{bmatrix} \frac{S_1 P_{g,1\to1}}{\Sigma_{T,g,1} V_1} & \frac{S_2 P_{g,2\to1}}{\Sigma_{T,g,1} V_1} & \frac{S_3 P_{g,3\to1}}{\Sigma_{T,g,1} V_1} & \frac{S_4 P_{g,4\to1}}{\Sigma_{T,g,1} V_1} \\ \frac{S_1 P_{g,1\to2}}{\Sigma_{T,g,2} V_2} & \frac{S_2 P_{g,2\to2}}{\Sigma_{T,g,2} V_2} & \frac{S_3 P_{g,3\to2}}{\Sigma_{T,g,2} V_2} & \frac{S_4 P_{g,4\to2}}{\Sigma_{T,g,2} V_2} \end{bmatrix} \quad (82)$$

A $\bar{\bar{S}}^I$ matrix may be created for each subsystem and hence the $\bar{\bar{S}}$ matrix will consist of blocks of $\bar{\bar{S}}^I$ on the diagonal and the rest of the matrix consisting of zeros:

$$\bar{\bar{S}} = \begin{bmatrix} S^1 & 0 & 0 \\ 0 & \ddots & 0 \\ 0 & 0 & S^n \end{bmatrix} \quad (83)$$

It is worth noting that the $\bar{\bar{S}}$ matrix for the whole system will not be a square matrix in all cases since it is dependent on the number of regions in each cell. The $\bar{\bar{S}}^I$ matrix will have dimensions of $(number\ of\ regions) \times 4$.

4.7 Calculating the F matrix

In order to calculate the new effective multiplication factor (k_{eff}) the power iteration method is used as shown before. The equations that is solved is equation 57:

$$k^{(p)} = k^{(p-1)} \times \frac{\bar{x}^{(p-1)} \cdot \bar{x}^{(p)}}{\bar{x}^{(p-1} \cdot \bar{x}^{(p-1)}}$$

where the $\bar{x}$ vector is given by:

$$\bar{x} = \bar{\bar{F}} \times \bar{\phi}$$

The $\bar{x}$ may be explicitly written for one region j and energy group g:

$$x_{g,j} = \sum_{i \in V_i} V_i Q_{g,i}^{fission} P_{g,i \to j} = \sum_{i \in V_i} V_i P_{g,i \to j} \chi_{g,i} \sum_{g'} (\nu \Sigma_f)_{g',i} \phi_{g',i} \tag{84}$$

Equation 84 may be expanded for a single region, fuel, and energy group, $g = 1$, as:

$$\begin{aligned} x_{1,fuel} = & V_{fuel} P_{1,fuel \to fuel} \chi_{1,fuel} (\nu \Sigma_{f,1,fuel}) \times \phi_{1,fuel} \\ & + V_{fuel} P_{1,fuel \to fuel} \chi_{1,fuel} (\nu \Sigma_{f,2,fuel}) \times \phi_{2,fuel} \\ & + V_{mod} P_{1,mod \to fuel} \chi_{1,mod} (\nu \Sigma_{f,1,mod}) \times \phi_{1,mod} \\ & + V_{mod} P_{1,mod \to fuel} \chi_{1,mod} (\nu \Sigma_{f,2,mod}) \times \phi_{2,mod} \end{aligned} \tag{85}$$

This may be done for any region in a cell and any group, and writing it in matrix form, the following equation is obtained:

$$\begin{bmatrix} x_{1,fuel} \\ x_{2,fuel} \\ x_{1,mod} \\ x_{2,mod} \end{bmatrix} = \bar{\bar{F}}^I \times \begin{bmatrix} \phi_{1,fuel} \\ \phi_{2,fuel} \\ \phi_{1,mod} \\ \phi_{2,mod} \end{bmatrix} \tag{86}$$

Where $\bar{\bar{F}}$ will contain the terms shown in equation 85 written for each region and group. The $\bar{\bar{F}}$ matrix simplifies since $\Sigma_{f,mod}$ will always be zero since there is no fission in moderator. For a single cell the $\bar{\bar{F}}^I$ will be a square 4×4 matrix when two regions are used. Similarly to the $\bar{\bar{S}}$ and $\bar{\bar{R}}$ matrices the $\bar{\bar{F}}$ matrix will consist of blocks of $\bar{\bar{F}}^I$ on the diagonal with rest of matrix containing zeros:

$$\bar{\bar{F}} = \begin{bmatrix} F^1 & 0 & 0 \\ 0 & \ddots & 0 \\ 0 & 0 & F^n \end{bmatrix} \tag{87}$$

4.8 Calculating emission density

In each region the emission density may be calculated according to:

$$Q_g^i = \frac{1}{4\pi} \sum_{g' \to 1}^{G} \left[\Sigma_{s0,g' \to g}^i + \frac{\chi_{g'}^i \nu \Sigma_{f,g'}^i}{k_{eff}} \right] \phi_{g'}^i \tag{88}$$

Which may be expanded for region i and a group g, in a two-group format, as:

$$Q_g^i = \frac{1}{4\pi} \left[\Sigma_{s0,1 \to g}^i \phi_1^i + \frac{\chi_1^i \nu \Sigma_{f,1}^i}{k_{eff}} \phi_1^i + \Sigma_{s0,2 \to g}^i \phi_2^i + \frac{\chi_2^i \nu \Sigma_{f,2}^i}{k_{eff}} \phi_2^i \right] \tag{89}$$

Once the emission density is determined in each region the source neutron flux contribution in each region may be calculated. In the moderator regions equation 89 will simplify since there is no fission and hence the second and fourth term will disappear.

4.9 Calculating source currents

In the global problem formulation the source current contribution needs to be calculated. The term may be seen in the equation below.

$$\bar{J}_{in} = \bar{\bar{P}} \times \bar{\bar{R}} \times \bar{J_{in}} + \bar{\bar{P}} \times \bar{J}_{source} \tag{90}$$

The coefficients needed to determine the source currents may be found in the explicit version of equation 90, without the introduction of the $\bar{\bar{P}}$ matrix:

$$S_a J_{out,g,a} = \sum_{b \in S_I} S_b J_{in,g,b} P_{g,b \to a} + \sum_{i \in V_I} V_i Q_{g,i} P_{g,i \to a} \tag{91}$$

The source current contribution to each surface current, for one cell, may be determined by:

$$\begin{bmatrix} J_{out,g,1} \\ J_{out,g,2} \\ J_{out,g,3} \\ J_{out,g,4} \end{bmatrix} = \begin{bmatrix} P_{g,1 \to 1} & P_{g,2 \to 1} \\ P_{g,1 \to 2} & P_{g,2 \to 2} \\ P_{g,1 \to 3} & P_{g,2 \to 3} \\ P_{g,1 \to 4} & P_{g,2 \to 4} \end{bmatrix} \times \begin{bmatrix} \frac{V_1}{S} & 0 \\ 0 & \frac{V_2}{S} \end{bmatrix} \times \begin{bmatrix} Q_1 \\ Q_2 \end{bmatrix} \tag{92}$$

and hence the source contribution to all out currents may be determined.

4.10 Calculating source flux

The source contribution to the neutron flux in each region needs to be determined. This may be done from equation 78. The source flux contribution will be given by:

$$\phi_{g,j}^{source} = \frac{\sum_{i \in V_I} V_i Q_{g,i} P_{g,i \to j}}{V_j \Sigma_{T,g,j}^0} \tag{93}$$

Which written explicitly gives:

$$\phi_{g,j}^{source} = \frac{V_i * Q_{g,i} P_{g,i \to j} + V_j * Q_{g,j} P_{g,j \to j}}{V_j \Sigma_{T,g,j}^0} \tag{94}$$

In the code this is calculated for one cell j as:

$$\bar{\phi}_{g,j}^{source} = \begin{bmatrix} \frac{V_i P_{g,i \to j}}{V_j \Sigma_{T,g,j}^0} & \frac{V_j P_{g,j \to j}}{V_j \Sigma_{T,g,j}^0} \\ \frac{V_i P_{g,i \to i}}{V_i \Sigma_{T,g,i}^0} & \frac{V_j P_{g,j \to i}}{V_i \Sigma_{T,g,i}^0} \end{bmatrix} \times \begin{bmatrix} Q_{i,g} \\ Q_{j,g} \end{bmatrix} \tag{95}$$

4.11 Cross-section data

In the build up of the different functions used in the deterministic MatLab code, a large number of cross-section data are used. Since a hybrid method is used, these data will also be taken from the Serpent2 results for each fuel pin. When Serpent2 has run a model it will give an output file with a large number of important parameters of which only a few are of importance to the response matrix method.

The data from the Serpent2 output files are computed for each fuel pin and stored in a cell array where they can be accessed by their associated pin and energy group.

5 Results and discussion

In the hybrid response matrix formulation two important results are calculated: the neutron flux in each region of the system and the neutron probabilities. Further the effective multiplication factor is also determined.

5.1 Probabilities

The Serpent2 runs will give the probabilities for neutrons and these are given for each different fuel pin. In the following tables the set of probabilities will be given for each pin and energy group.

Table 7: Sets of probabilities for neutrons emitted from fuel (i). First the fast energy group is given and then the thermal group.

Pin	$P_{i\to i}$	$P_{i\to j}$	$P_{i\to a_1}$	$P_{i\to a_2}$	$P_{i\to a_3}$	$P_{i\to a_4}$	Sum
1	0.2148	0.1380	0.1618	0.1618	0.1618	0.1618	1.0000
2	0.2140	0.1384	0.1619	0.1619	0.1619	0.1619	1.0000
3	0.2147	0.1379	0.1619	0.1619	0.1619	0.1619	1.0000
4	0.2140	0.1383	0.1619	0.1619	0.1619	0.1619	1.0000
5	0.2154	0.1381	0.1616	0.1616	0.1616	0.1616	1.0000
6	0.2137	0.1381	0.1620	0.1620	0.1620	0.1620	1.0000
1	0.2453	0.2874	0.1168	0.1168	0.1168	0.1168	1.0000
2	0.2523	0.2846	0.1158	0.1158	0.1158	0.1158	1.0000
3	0.2615	0.2785	0.1150	0.1150	0.1150	0.1150	1.0000
4	0.2710	0.2742	0.1137	0.1137	0.1137	0.1137	1.0000
5	0.2755	0.2709	0.1134	0.1134	0.1134	0.1134	1.0000
6	0.2801	0.2686	0.1128	0.1128	0.1128	0.1128	1.0000

In table 7 some trends may be identified. With increasing enrichment it can be seen that the probability for neutrons to go from fuel to fuel in the thermal group increases, with increasing enrichment the amount of U-235 increases which has a larger fission cross-section and hence also total cross-section. The change in cross-sections for all pins and groups, calculated by Serpent2, may be seen in table 8.

This means that more fission will take place and the probability for a neutron to be absorbed in the fuel increases. Following this trend it may be seen that the probability for a neutron to go from fuel to moderator will act inversely since fewer neutrons will escape from the fuel. Since the likelihood for neutrons to escape the fuel decreases it is also plausible that the probability for neutrons to escape to a surface decreases with increasing enrichment. These trends are not seen in the fast energy groups since the mean free path length for fast neutrons is much longer and hence less affected by the change in enrichment. These observations may

Table 8: The fission and total cross-section, for fuel, given for each fuel pin, for the fast and thermal energy groups respectively.

Pin	Σ_f	Σ_{tot}
1	0.0156	0.4229
2	0.0170	0.4236
3	0.0191	0.4243
4	0.0208	0.4249
5	0.0224	0.4257
6	0.0236	0.4260
1	0.2853	0.5732
2	0.3264	0.5926
3	0.3931	0.6243
4	0.4447	0.6489
5	0.4940	0.6724
6	0.5301	0.6897

agree with the way a probability would be calculated by the interface current method in equation 96 and 97:

$$P_{i\to j} = \frac{\Sigma^0_{T,j}(E)}{V_i} \int_{V_i} dV' \int_{V_j} \frac{exp[-\tau(r',r,E)]}{4\pi\|r-r'\|^2} dV \tag{96}$$

$$P_{i\to a} = \frac{\int_{S_a} \left|\bar{\Omega}\cdot\bar{n}\right| dS \int_{V_j} Q(r',E) \frac{exp[-\tau(r,r',E)]}{4\pi\|r-r'\|^2} dV'}{V_i \int_{V_i} Q(r,E) dV} \tag{97}$$

where it can be seen that the only terms that are affected by the change in enrichment is the total cross-section and hence also the exponential function of the optical path length. These two terms change magnitude in opposite directions. Since these are the only two terms changing it may be suggested that the change in total cross-section in the optical path length has a smaller effect than when multiplying directly the integrals with the total cross-section. Hence leading to a larger probability for fuel to fuel when the enrichment increases.

In the case for neutrons emitted from the moderator it can be seen in table 9 that the probability for neutrons to go from moderator to moderator increases with increasing enrichment. This change is harder to interpret since the probability terms are affected by the total cross-section of both the fuel and the moderator. However, it can be seen that the total cross-section for the moderator increases with increasing enrichment, which would directly increase the probability through multiplication by the integrals in equation 96.

Table 9: Sets of probabilities for neutrons emitted from moderator (j). First the fast neutron group is given and then the thermal group.

Pin	$P_{j\to j}$	$P_{j\to i}$	$P_{j\to a_1}$	$P_{j\to a_2}$	$P_{j\to a_3}$	$P_{j\to a_4}$	Sum
1	0.2582	0.0779	0.1652	0.1652	0.1656	0.1652	0.9973
2	0.2668	0.0784	0.1654	0.1652	0.1654	0.1656	1.0067
3	0.2780	0.0785	0.1654	0.1657	0.1657	0.1657	1.0188
4	0.2853	0.0790	0.1655	0.1656	0.1658	0.1658	1.0269
5	0.2912	0.0792	0.1658	0.1656	0.1659	0.1657	1.0334
6	0.2951	0.0794	0.1658	0.1659	0.1661	0.1658	1.0381
1	0.4168	0.0801	0.1320	0.1317	0.1319	0.1318	1.0243
2	0.4170	0.0827	0.1318	0.1318	0.1320	0.1316	1.0268
3	0.4173	0.0862	0.1318	0.1318	0.1320	0.1317	1.0309
4	0.4182	0.0890	0.1319	0.1316	0.1314	0.1319	1.0340
5	0.4193	0.0918	0.1315	0.1314	0.1315	0.1315	1.0370
6	0.4193	0.0939	0.1316	0.1314	0.1315	0.1317	1.0393

Table 10: The total cross-section, for the moderator, given for each fuel pin, for the fast and thermal energy groups respectively.

Pin	Σ_{tot}
1	0.4065
2	0.4058
3	0.4045
4	0.4036
5	0.4029
6	0.4020
1	1.1163
2	1.1072
3	1.0941
4	1.0851
5	1.0766
6	1.0709

In table 11 some trends may be identified, these trends are more explicit in the thermal energy group due to the shorter mean path of these neutrons than for the fast neutrons:

- With increasing enrichment the probabilities to go from surface to any surface decreases. This is due to the enrichment leading to a larger fission cross-section in the fuel which

Table 11: Sets of probabilities for neutrons entering through any surface (a_1). First the fast neutron group is given and then the thermal group.

Pin	$P_{a_1 \to a_1}$	$P_{a_1 \to a_2}$	$P_{a_1 \to a_3}$	$P_{a_1 \to a_4}$	$P_{a_i \to fuel}$	$P_{a_1 \to moderator}$	Sum
1	0	0.2170	0.2101	0.2097	0.1247	0.2385	1.0000
2	0	0.2172	0.2100	0.2100	0.1250	0.2378	1.0000
3	0	0.2173	0.2101	0.2101	0.1252	0.2373	1.0000
4	0	0.2174	0.2102	0.2104	0.1254	0.2366	1.0000
5	0	0.2176	0.2103	0.2105	0.1254	0.2362	1.0000
6	0	0.2173	0.2105	0.2104	0.1258	0.2360	1.0000
1	0	0.1078	0.1334	0.1336	0.1221	0.5031	1.0000
2	0	0.1081	0.1344	0.1338	0.1251	0.4987	1.0000
3	0	0.1061	0.1349	0.1344	0.1309	0.4938	1.0000
4	0	0.1048	0.1347	0.1352	0.1345	0.4908	1.0000
5	0	0.1037	0.1346	0.1347	0.1390	0.4880	1.0000
6	0	0.1034	0.1349	0.1346	0.1418	0.4853	1.0000

means more neutrons will be absorbed in the fuel leading to fewer escaping to another surface. This effect is seen in the optical path length in equation 98

- The probability to go from surface to fuel increases with increasing enrichment since the fission cross-section will lead to a larger number of neutrons being absorbed in the fuel.
- Inversely to the previous trend the probability for neutrons to go from a surface to moderator decreases since more neutrons will be absorbed in the fuel rather than in the moderator.

The surface to surface probability term would be calculated according to:

$$P_{b \to a} = \frac{\int_{S_a} \left|\bar{\Omega} \cdot \bar{n}\right| dS \int_{S_b} \Psi(r', \bar{\Omega}, E) \frac{exp[-\tau(r,r',E)]}{4\pi \|r - r'\|^2} \left|\bar{\Omega} \cdot \bar{n}\right| dS'}{S_b J_{in,b}(E)} \tag{98}$$

where it may be seen that increasing the total cross-sections, as happens when the enrichment is increased, the optical path length decreases and hence also the probability.

5.2 Neutron flux

Once the deterministic solver has converged the neutron flux in each region of the fuel assembly has been determined. Taking the neutron fluxes in each region on the diagonal of the fuel assembly produces the graph in figure 9:

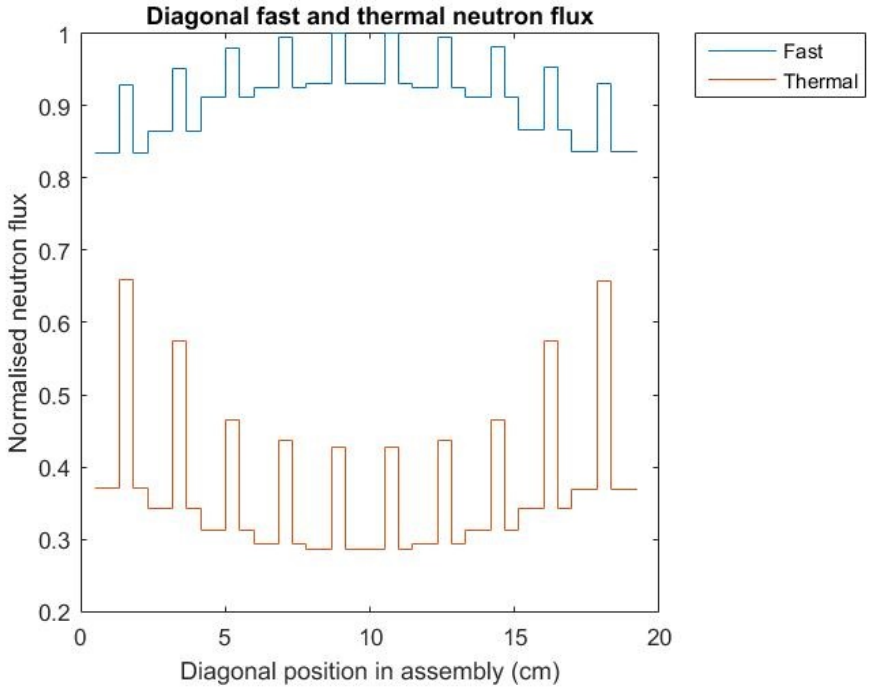


Figure 9: The fast and thermal neutron flux plotted for the diagonal through the assembly.

In figure 9 the peaks that may be identified are regions of fuel and the two values around each peak is the neutron flux determined for the moderator around the associated fuel region. The moderator neutron flux next to each fuel region are identical since they are taken from the same moderator region. In a more detailed solution strategy the moderator region could be split up into further regions.

The general shape of the graphs for the fast and thermal neutron fluxes may be explained by the placement of fuel pins in the assembly. It is a symmetrical assembly which looks as following:

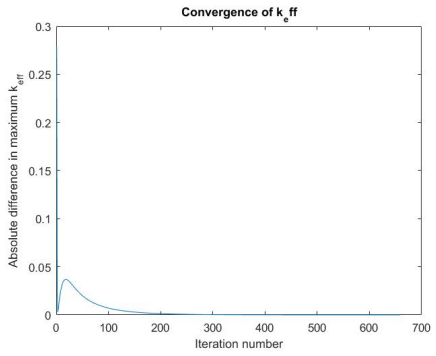
$$\begin{bmatrix} 2 & 2 & 3 & 5 & 5 & 5 & 5 & 3 & 2 & 2 \\ 2 & 3 & 5 & 6 & 6 & 6 & 6 & 5 & 3 & 2 \\ 3 & 5 & 6 & 6 & 6 & 6 & 6 & 6 & 5 & 3 \\ 5 & 6 & 6 & 6 & 6 & 6 & 6 & 6 & 6 & 5 \\ 5 & 6 & 6 & 6 & 6 & 6 & 6 & 6 & 6 & 5 \\ 5 & 6 & 6 & 6 & 6 & 6 & 6 & 6 & 6 & 5 \\ 5 & 6 & 6 & 6 & 6 & 6 & 6 & 6 & 6 & 5 \\ 3 & 5 & 6 & 6 & 6 & 6 & 6 & 6 & 5 & 3 \\ 2 & 3 & 5 & 6 & 6 & 6 & 6 & 5 & 3 & 2 \\ 2 & 2 & 3 & 5 & 5 & 5 & 5 & 3 & 2 & 2 \end{bmatrix} \tag{99}$$

It may be seen that there is a concentration of fuels pins with high enrichment, pin 6, in

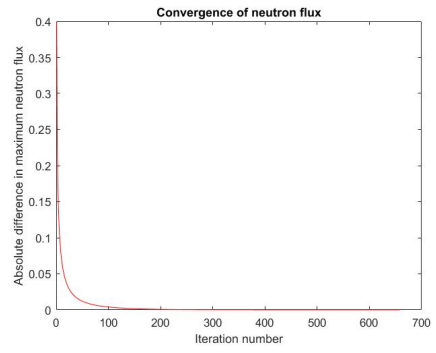
the centre of the assembly. This will lead to a larger number of neutrons being produced in the centre of the assembly, due to fission, leading to a larger number of fast neutrons in this region. This may also been seen in figure 9 where the fast relative neutron flux is higher in the middle. Inversely the thermal neutron flux is relatively low in the middle of the assembly due to the higher absorption of neutrons at thermal energies.

The neutron flux flattens out towards the edges of the system may be explained by the boundary conditions. Since a reflective boundary condition is used, the net-neutron current across the boundary is zero, resulting in a flat flux distribution. Since the neutron flux is related to the derivative of the neutron current the neutron flux will flatten out.

Further the effective multiplication factor was determined using the power iteration method. For the symmetrical assembly used, k_{eff} was determined to be 13.8 which is an unphysical results. The deterministic solver converged to this k_{eff} and neutron flux distribution in 658 iterations. Both the neutron flux and k_{eff} converged to a relative difference smaller than 1E-6 as may be seen in figure 10. The reason for this unphysical result is unknown and runs with a identical system in Serpent2 yielded a k_{eff} of approximately 1.15.



(a) The convergence in k_{eff}.



(b) The convergence of the neutron flux.

Figure 10: The convergence of k_{eff} and the neutron flux.

5.3 Conclusion and outlook

The response matrix formulation method was used to calculate the neutron flux in a simple BWR fuel assembly, however, determination of a physical result for the effective multiplication factor was not achieved. The error in the calculation of the effective multiplication factor is unknown and would need to be solved to have a complete solution. In the calculation of the probabilities used, a better understanding is required with respect to the handling of source neutrons for scattering within a region in Serpent2. Further the method can be improved by using more regions for both fuel and moderator, as well as calculating the probabilities for any fuel pin, even those surrounded or close to a water hole.

6 Bibliography

[1] S. E. Agency, Energiläget 2015, http://www.energimyndigheten.se/en/ (2015).

[2] R. de transport d'électricité, Annual electricity report france, http://www.rte-france.com/en (2015).

[3] C. Demazière, Multi-physics modelling of nuclear reactors: current practices in a nutshell, Int. J. Nuclear Energy Science and Technology 7 (4) (2013) 288–318.

[4] C. Demazière, Physics of Nuclear Reactors, Division of Nuclear Engineering, 2014.

[5] M. J. Lee, H. G. Joo, D. Lee, Coarse mesh finite difference formulation for accelerated monte-carlo eigenvalue calculation, Annals of Nuclear Energy 65 (2014) 101–113.

[6] D. Zhang, F. Rahnema, An efficient hybrid stochastic/deterministic coarse mesh neutron transport method, Annals of Nuclear Energy 41.

[7] S. Mosher, F. Rahnema, The incident flux response expansion method for heterogeneous coarse mesh transport problems, Transport Theory and Statistical Physics 35.

[8] C. Demazière, Modelling of Nuclear Reactors, Division of Nuclear Engineering, 2016.

[9] VTT, Serpent wiki, `http://serpent.vtt.fi/mediawiki/index.php/Collection_of_example_input_files` (2 2017).

[10] VTT, Serpent wiki, `http://serpent.vtt.fi/mediawiki/index.php/Main_Page` (11 2016).